VOL. 191, NO. 5 THE AMERICAN NATURALIST MAY 2018

Host Traits Drive Viral Life Histories across Phytoplankton Viruses

Kyle F. Edwards* and Grieg F. Steward

Department of Oceanography, University of Hawai'i at Mānoa, Honolulu, Hawaii 96822

Submitted May 9, 2017; Accepted November 15, 2017; Electronically published March 16, 2018

Online enhancements: supplemental material. *Dryad data*:http://dx.doi.org/10.5061/dryad.31sm2.

ABSTRACT: Viruses are integral to ecological and evolutionary processes, but we have a poor understanding of what drives variation in key traits across diverse viruses. For lytic viruses, burst size, latent period, and genome size are primary characteristics controlling host-virus dynamics. Here we synthesize data on these traits for 75 strains of phytoplankton viruses, which play an important role in global biogeochemistry. We find that primary traits of the host (genome size, growth rate) explain 40%–50% of variation in burst size and latent period. Specifically, burst size and latent period both exhibit saturating relationships versus the host : virus genome size ratio, with both traits increasing at low genome size ratios while showing no relationship at high size ratios. In addition, latent period declines as host growth rate increases. We analyze a model of latent period evolution to explore mechanisms that could cause these patterns. The model predicts that burst size may often be set by the host genomic resources available for viral construction, while latent period evolves to permit this maximal burst size, modulated by host metabolic rate. These results suggest that general mechanisms may underlie the evolution of diverse viruses. Future extensions of this work could help explain viral regulation of host populations, viral influence on community structure and diversity, and viral roles in biogeochemical cycles.

Keywords: burst size, latent period, genome size, evolution, adaptive dynamics, microbe.

Introduction

Viruses are integral to the ecology and evolution of all cellular life (Villarreal and Witzany 2010; Koonin and Dolja 2013). By selectively lysing or altering the physiology of the cells they infect and mediating horizontal gene transfer among genetically distinct lineages, they can generate and maintain host diversity and influence biogeochemical cycles (Suttle 2007; Breitbart 2012). Viruses are highly host specific and exhibit great taxonomic and genetic diversity, with many forms still being discovered and characterized (Lang et al. 2009; Rosario et al. 2012; Fischer 2016). Although viruses were discovered more than a century ago and some model systems have been studied in great detail, we have a poor understanding of what drives variation in key traits across diverse viruses. Research on functional trait diversity has been fruitful in linking physiology, community structure, and ecosystem dynamics, particularly in terrestrial plants (Westoby and Wright 2006) and phytoplankton (Litchman and Klausmeier 2008). If broad patterns and mechanisms underlying how viruses function can be discerned, this will promote a general framework for predicting viral ecology and the effects of viral interactions on host populations, communities, and ecosystems (Gudelj et al. 2010). In this study, we examine viruses that infect phytoplankton, a group of viruses that have a direct influence on one of the most important biogeochemical transformations on the planet. Phytoplankton account for nearly half of global primary production and participate in multiple elemental cycles (Falkowski et al. 2004). Viral effects on mortality, element cycling, and community structure of phytoplankton potentially have global consequences (Brussaard 2004; Weitz et al. 2015).

We will focus on several traits of lytic viruses. Lytic viruses always produce virions and lyse the host cell, provided the cell has sufficient resources and integrity to support the infection. Viruses replicating via the lytic cycle can have particularly dramatic effects on host populations because of their rapid rate of population growth and corresponding destruction of the host population. Key traits of lytic viruses include burst size (new virions produced per infected host), latent period (time elapsed between infection and lysis), and viral genome size. Burst size and latent period are analogous to the organismal life-history traits of fecundity and generation time and are key parameters for host-virus population dynamics. The burst size and latent period of a virus can vary with environmental conditions or host genotype (Wilson et al. 1996; Maat and Brussaard 2016), but these parameters also vary greatly among different viral strains

* Corresponding author; e-mail: kfe@hawaii.edu.
ORCID: Steward, http://orcid.org/0000-0001-5988-0522.

Am. Nat. 2018. Vol. 191, pp. 566–581.
0003-0147/2018/19105-57713$15.00.
DOI: 10.1086/696849

measured under similar conditions (typically, resource-replete exponential growth of the host). For simplicity, we will refer to differences across isolates as variation in viral traits, although such differences are likely driven by both viral genotype and host genotype. Viral genome size is a trait that will affect viral control of host metabolism, as well as virion size and the metabolic cost of synthesizing new virions (Bragg and Chisholm 2008; Thomas et al. 2011; Steward et al. 2013). Here we analyze variation in burst size, latent period, and genome size across viruses. We focus on these traits because they are important and have been quantified for numerous isolates that infect phytoplankton and other unicellular algae.

Guided by previous work, we can make predictions about drivers of variation in these traits: conditions that may select for particular trait values and constraints that may cause the traits to covary. Viruses use their host's molecular machinery to reproduce, and therefore host structure and physiology are primary selective forces for viral trait evolution. Nucleotides for viral genome synthesis come from host nucleotide pools and degradation of the host genome, with an uncertain and variable contribution of de novo nucleotide synthesis during infection (Van Etten et al. 1984; Wikner et al. 1993; Brown et al. 2007; Thompson et al. 2011). Host genome size may thus influence the rate of viral production or burst size. A prior synthesis of 15 host-virus pairs found that viral nucleotide production correlates with host genome size (Brown et al. 2006). The growth rate of the host will likely correlate with the concentration of ribosomes and enzymes required to synthesize host proteins, RNA, and DNA, which are also used to construct new virus particles (You et al. 2002; Daines et al. 2014). Therefore, host growth rate may also affect the rate of viral production.

Within the context set by host conditions, viral traits should evolve to maximize fitness. Burst size and latent period are intrinsically related, because lysing the host sooner will reduce burst size, all else being equal. Theory and experiments with *E. coli* show that the optimal latent period (and burst size) depends on host density and quality, such that a shorter latent period is selected for when hosts are more dense or of higher quality (Wang et al. 1996; Abedon et al. 2003). However, these models and experiments assume that host density is relatively constant, rather than being regulated by the virus. If the virus suppresses host density, this may alter the optimal latent period, and evolution of latent period (and burst size) may then feed back to alter the strength of top-down effects. Therefore, eco-evolutionary dynamics (Fussmann et al. 2007) are likely to be important for explaining why life-history traits vary across viruses. Models that include bacteriophage-host dynamics and latent period evolution have been developed recently (Bonachela and Levin 2014). To ask how patterns of viral trait diversity might emerge, we can model latent period evolution across realistically diverse selective pressures (host genome size and growth rate, viral genome size, viral decay rate, etc.). We can then ask whether empirical patterns of trait variation are consistent with theoretical expectations for particular mechanisms.

Our approach in this study combines data synthesis and theory to understand viral trait diversity. First, we compile experimental studies to explore variation across microalgal viruses in burst size and latent period and ask how these traits correlate with one another and with other virus and host traits (genome sizes, growth rates). The reasoning outlined above leads to some general hypotheses: burst size and latent period will tend to be positively correlated, and both traits may be modulated by (1) the genome size of the host (larger hosts may permit a larger optimal burst size); (2) the growth rate of the host (faster growth may decrease optimal latent period); and (3) the genome size of the virus (larger viruses require more resources per virion, which may reduce optimal burst size). Second, we model latent period evolution, to predict in more detail how selective pressures will cause these traits to covary across host-virus systems. This is important because multiple selective pressures vary simultaneously across the environments that viruses experience. A model allows us to ask which patterns of trait variation and covariation will tend to emerge robustly, which relationships will be weak or absent, and what mechanisms are responsible. In the text that follows, methods and results for the data synthesis are presented first, followed by methods and results for the model developed to explain the empirical patterns. Figures 1 and 2 include both empirical and model results for ease of comparison.

Methods: Data Synthesis

Virus Trait Compilation

The literature was searched for studies that measured burst size and latent period of viruses isolated on phytoplankton or other microalgal hosts (table S1, available online; data available in the Dryad Digital Repository: http://dx.doi.org/10.5061/dryad.31sm2 [Edwards and Steward 2018]). We included only experiments where the host was grown under nutrient-replete conditions, so that we could quantify functional variation across viruses cultured under similar conditions, as opposed to plastic responses of individual strains. We recorded the name of the virus strain, virus genome type (dsDNA/dsRNA/ssDNA/ssRNA), virus source location, host species, host taxon (chlorophyte/cryptophyte/cyanobacterium/diatom/dinoflagellate/haptophyte/pelagophyte/raphidophyte), and environment (marine/freshwater). We also recorded whether burst size was estimated by counting infectious units or free virions. Virus capsid size (diameter) and genome size estimates were taken from the same study or other studies on

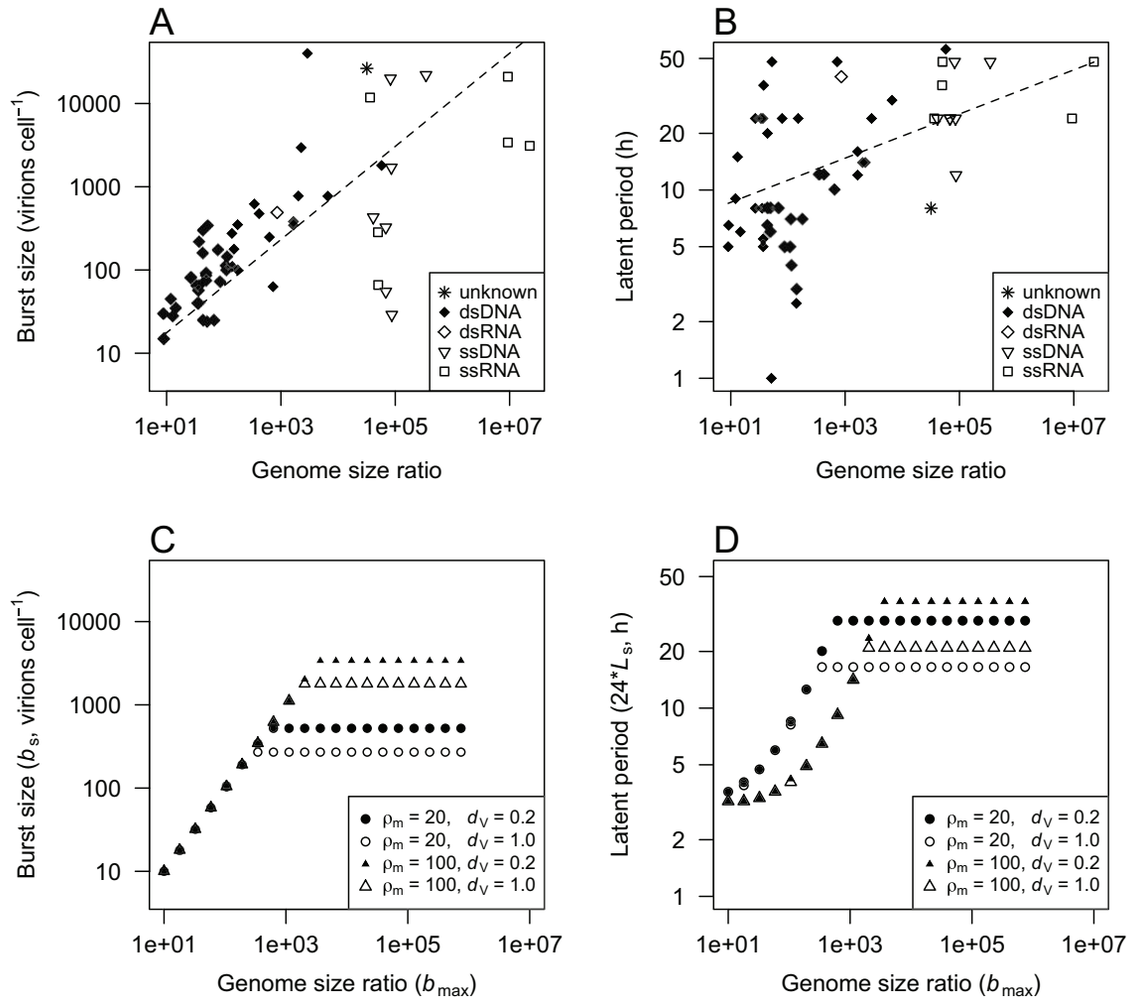

Figure 1: Relationships between viral traits and the genome size ratio (host genome size/viral genome size). *A*, *B*, Empirical patterns. *C*, *D*, Model results for the same relationships. *A*, Burst size versus the genome size ratio. *B*, Latent period versus the genome size ratio. *C*, Model burst size (b_s) versus genome size ratio (b_{max}). *D*, Model latent period (L_s) versus genome size ratio (b_{max}). Here L_s is the latent period of the genotype selected for in the model and b_s is the corresponding burst size (when host growth rate = μ_{max}). *A*, *B*, Dashed lines show fitted relationships for all strains, from mixed models in which host genus, host taxon, virus type, and publication were included as random effects. *C*, *D*, Results are shown when varying two parameters: ρ_m, which controls the rate of virion production; and d_V, the virion decay rate (d^{-1}). These parameters were chosen because they have large effects on evolutionary outcomes; effects of additional parameters are in the supplementary figures. Host maximum growth rate $\mu_{max} = 1$ (d^{-1}) in all cases; other parameters are assigned the values in table 1.

the same isolate. Virus genome size correlates strongly with capsid diameter, and thus we use only genome size to represent virus size in all analyses (fig. S1*A*; figs. S1–S3 are available online). For some analyses, we quantify total viral nucleotide output at lysis (burst size × virus genome size); for these calculations, we divided the genome size of the single-stranded viruses by a factor of 2. Host genome size and cell volume estimates were taken from the literature, and if an estimate for the host species was not available, an estimate from a congener was used if available. It is noteworthy that 10 of the 13 single-stranded viruses have been isolated from *Chaetoceros* species, and in the absence of published information on genome sizes for most of the hosts, we assigned all of the host species the same genome size (measured for *Chaetoceros muelleri*). For the double-stranded viruses, genome size estimates were available for nearly all host species. When possible, host exponential growth rate was estimated using DataThief (Tummers 2006) to extract growth curves measured on uninfected hosts or hosts growing prior to infection. Temperature and irradiance under which the hosts were cultured during one-step growth experiments were also recorded.

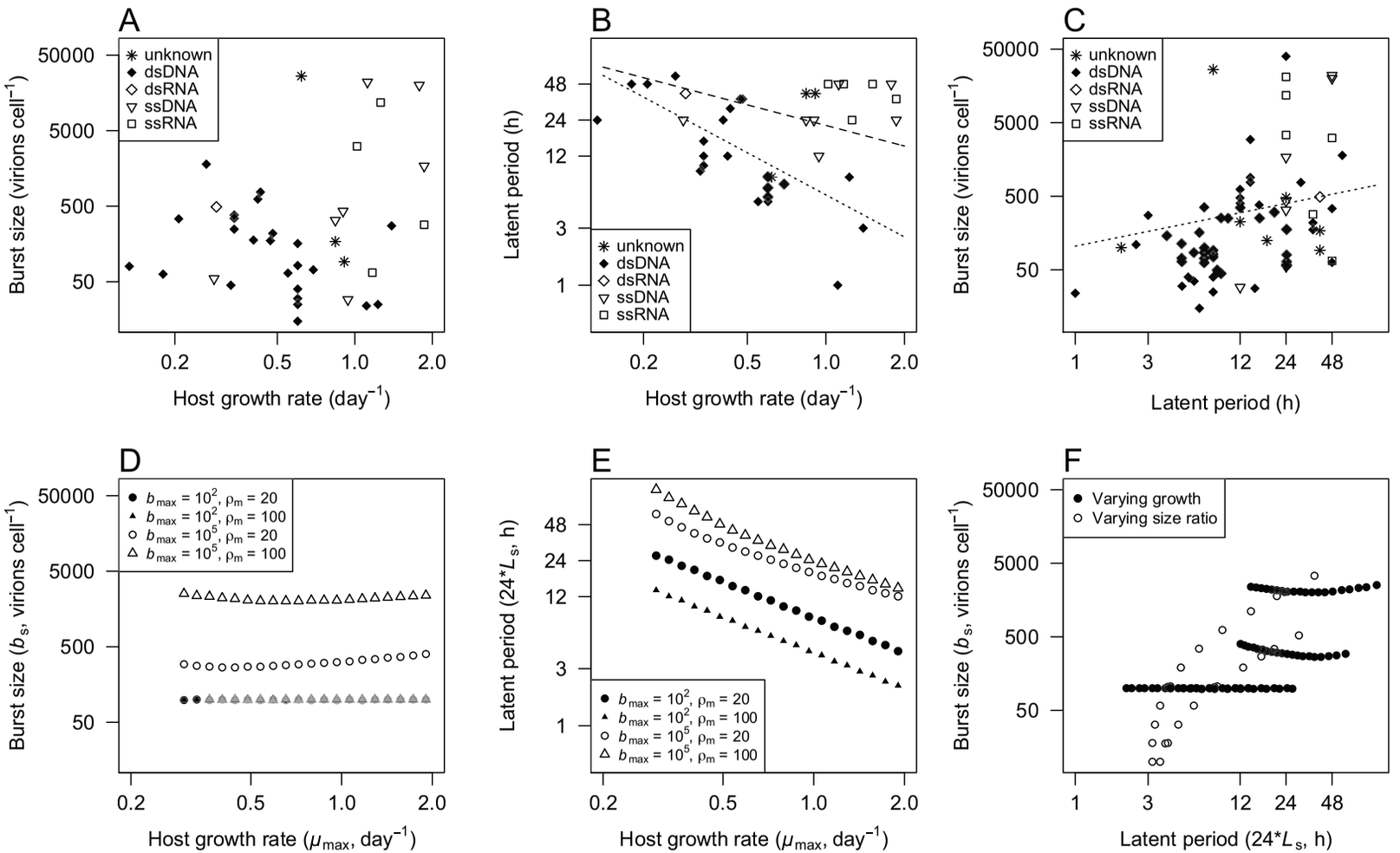

Figure 2: Relationships between viral traits and host growth rate. *A–C*, Empirical patterns. *D–F*, Model results for the same relationships. *A*, Burst size versus host growth rate. *B*, Latent period versus host growth rate. *C*, Burst size versus latent period. *D*, Model burst size (b_s) versus host growth rate (μ_{max}). *E*, Model latent period (L_s) versus host growth rate (μ_{max}). *F*, Model burst size (b_s) versus latent period (L_s). Here L_s is the latent period of the genotype selected for in the model, and b_s is the corresponding burst size (when host growth rate $= \mu_{max}$). *A–C*, Dashed lines show fitted relationships for all strains and dotted lines show fitted relationships for dsDNA viruses from mixed models in which host genus, host taxon, virus type, and publication were included as random effects. *D–E*, Results are shown when varying two parameters: b_{max}, the maximum possible burst size (=genome size ratio); and ρ_m, which controls the rate of virion production. These parameters were chosen because they have large effects on evolutionary outcomes; effects of additional parameters are in the supplementary figures. In *F*, two kinds of model output are combined: output when varying genome size ratio (fig. 1*C*, 1*D*) and output when varying host growth rate (fig. 2*D*, 2*E*). This displays how burst size and latent period are predicted to covary over a range of environmental conditions. Viral decay rate $d_V = 0.7$ (d^{-1}); other parameters are assigned the values in table 1.

Statistical Methods

Relationships between viral traits, or viral traits and host traits, were analyzed using mixed models (R package lme4; Bates et al. 2015). We used random effects to appropriately account for nonindependence in the data resulting from multiple viruses infecting similar hosts (host genus), multiple viruses measured in the same study (study ID), host taxonomy (diatom/cyanobacteria/haptophyte/etc.), or similarities among virus type (dsDNA/dsRNA/ssDNA/ssRNA). These random effects were included in all models, and different fixed effects and response variables were used to test different relationships (e.g., host genome size as a predictor of burst size). Significance of fixed effects was tested using approximate *F* tests (R package lmerTest; Kuznetsova et al. 2016), and variation explained by fixed effects was quantified as marginal R^2_{GLMM} (R package MuMIn; Bartón 2016). Preliminary results showed that patterns did not vary between marine and freshwater strains or between estimates of burst size using infectious units versus direct counts; therefore, these factors were excluded from the analyses for simplicity.

Results: Data Synthesis

Compilation

The literature compilation yielded data on 75 unique virus strains, including 51 dsDNA, 1 dsRNA, 7 ssDNA, and 6 ssRNA viruses and 12 viruses of unknown type (table S1). The viruses were isolated from 26 phytoplankton genera, with 38 strains isolated from cyanobacteria, 15 from diatoms, 10 from haptophytes, 7 from chlorophytes, 4 from dinoflagellates, and 1 each from a cryptophyte, raphidophyte, and pelagophyte. The majority was isolated from marine systems (58 vs. 19 from fresh waters). The genome size of the isolates ranges from 4.4 to 560 kb, and capsid diameter ranges from 22 to 310 nm. In our analyses, we consider relationships across all viruses as well as relationships within the dsDNA viruses, which are the most numerous and sometimes show distinct patterns compared to single-stranded viruses.

Empirical Trait Relationships

We tested a variety of hypothesized correlations between viral traits and between viral and host traits. In brief, burst size is most strongly related to the ratio (host genome size)/(viral genome size), which we refer to as the genome size ratio. Latent period is most strongly related to a combination of host growth rate and the genome size ratio. Figure 1*A* shows that burst size ranges over four orders of magnitude and that a larger genome size ratio is correlated with a greater burst size. The genome size ratio can explain half of the variation in burst size ($R^2 = 0.49$, $F_{1,44} = 33$, $P < .001$), and the relationship is strongest for dsDNA viruses, with greater variability for the single-stranded viruses that infect diatoms. A similar pattern is found when comparing total viral nucleotide output to host genome size (fig. S1*B*; $R^2 = 0.54$, $F_{1,5} = 16$, $P = .01$); for dsDNA viruses, these quantities tend to be directly proportional, which means that the number of nucleotides in released virions is similar to the number in the host genome. Latent period also increases with the genome size ratio, though less steeply than burst size (fig. 1*B*; $R^2 = 0.30$, $F_{1,14} = 9.3$, $P = .008$).

In contrast to genome size ratio, growth rate of the host has qualitatively distinct relationships with burst size and latent period. Burst size is unrelated to host growth rate (fig. 2*A*). For dsDNA viruses, there is a fairly strong relationship between host growth rate and latent period, with latent period declining about 10-fold for a 10-fold increase in host growth rate and latent period roughly equal to half of the host doubling time (fig. 2*B*, dotted line; $R^2 = 0.47$, $F_{1,9} = 29$, $P < .001$). This pattern is weaker when single-stranded viruses are included (fig. 2*B*, dashed line; $R^2 = 0.14$, $F_{1,20} = 6.6$, $P = .02$). In a multivariate model, both genome size ratio and host growth rate are significant predictors of latent period, and they jointly explain 38% of variation in latent period across all viruses and 57% of variation for dsDNA viruses. When comparing burst size and latent period directly, they are weakly positively correlated but only within the dsDNA strains; this corresponds to a 5-fold increase in burst size across a 50-fold increase in latent period (fig. 2*C*; $R^2 = 0.05$, $F_{1,22} = 4.6$, $P = .043$).

In contrast to genome size ratio, viral genome size alone is a poor predictor of viral traits. There is a moderate tendency for larger viruses to have a smaller burst size when comparing all strains, corresponding to a ~100-fold decrease in burst size over a 100-fold increase in genome size (fig. 3*A*; $R^2 = 0.2$, $F_{1,20} = 11.7$, $P = .003$). This pattern is driven by the difference between single-stranded and double-stranded strains. Latent period is unrelated to viral genome size (fig. 3*B*). There is also no overall relationship between host genome size and viral genome size when looking at all viruses or only dsDNA viruses (fig. 3*C*). However, it is noteworthy that the smallest viruses, which are single stranded, have so far been isolated only from relatively large eukaryotes (fig. 3*C*).

Methods: Model of Viral Life-History Evolution

The data synthesis showed that much of the variation in viral traits can be explained by traits of the host, with burst size explained by the genome size ratio (fig. 1*A*) and latent period explained by the genome size ratio as well as host growth rate (figs. 1*B*, 2*B*). Furthermore, some traits are uncorrelated or weakly correlated, such as burst size and

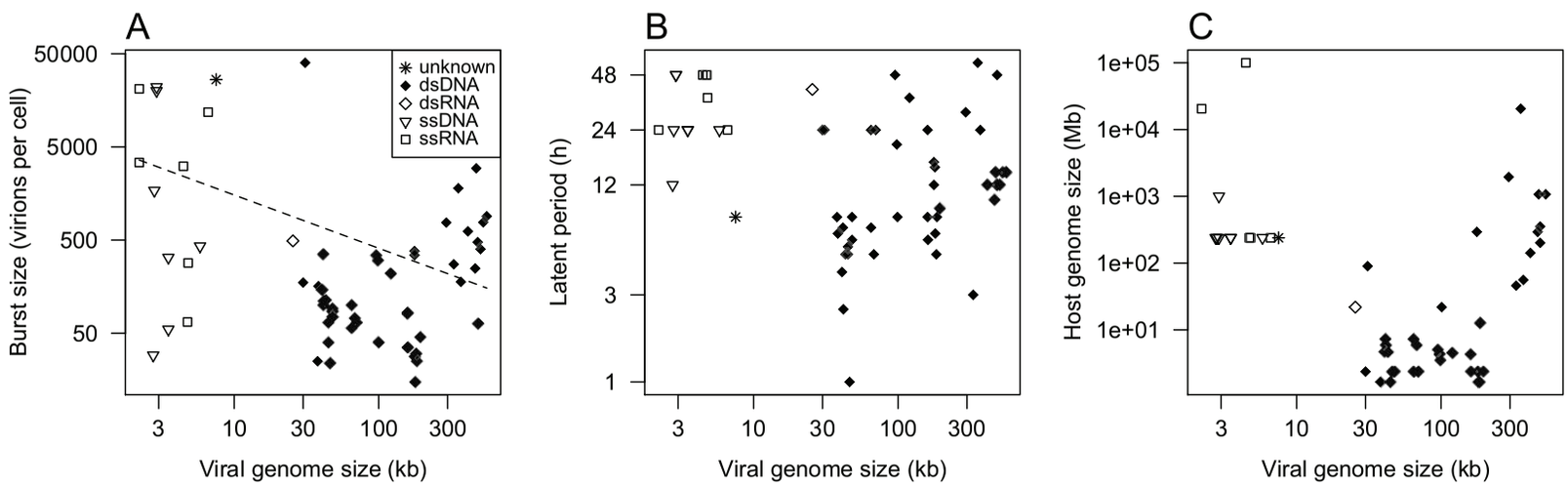

Figure 3: Relationships with viral genome size. *A*, Burst size versus viral genome size. *B*, Latent period versus viral genome size. *C*, Host genome size versus viral genome size. The dashed line shows the fitted relationship for all strains from a mixed model in which host genus, host taxon, virus type, and publication were included as random effects. These empirical patterns are shown without a model comparison because the model did not include viral genome size as an independent parameter, instead focusing on the genome size ratio as a driver of trait diversity.

latent period (fig. 2*C*). To gain further insight into why some traits exhibit substantial correlation while others show little correlation, we analyze a model of viral trait evolution. Specifically, we ask whether these patterns of trait covariation are expected to evolve due to two hypothesized mechanisms: (1) viral production is constrained by host genomic resources, and hosts vary in genome size; and (2) the rate of viral production is proportional to host growth rate, and hosts vary in their growth rate. The model is adapted from previous work on bacteriophage (Levin et al. 1977; Bonachela and Levin 2014), and the contribution of our analysis is to test the effect of parameters representing host growth and genome size. The model can be written as follows:

$$\frac{dP}{dt} = \frac{\mu_{\max} PN}{h + N} - \sum_i ckPV_i - d_P P + m(P_{\text{in}} - P), \quad (1)$$

$$\frac{dI}{dt} = \sum_i ckPV_i - \sum_i ckV_i^{t-L_i} P^{t-L_i} e^{-(d_P+m)L_i} - d_P I - mI, \quad (2)$$

$$\frac{dV_i}{dt} = b_i ckV_i^{t-L_i} P^{t-L_i} e^{-(d_P+m)L_i} - kV_i P - d_V V_i - mV_i, \quad (3)$$

$$\frac{dN}{dt} = m(N_{\text{in}} - N) - q\frac{\mu_{\max} PN}{h + N}. \quad (4)$$

The model explicitly represents latent period as a delay between infection and production of new virions (Levin et al. 1977; Bonachela and Levin 2014). In equation (1), susceptible phytoplankton (P) grow at a rate $\mu_{\max} PN/(h + N)$, limited by nutrient (N), with maximum growth rate $\mu_{\max}$ and half-saturation constant h. Susceptible hosts are lost due to infection at a rate of $\sum_i ckPV_i$, with infection from each viral strain i (V_i) and adsorption rate k. Here k represents the adsorption rate of successful infections and can be considered an effective adsorption rate. The conversion factor c ensures equations (1)–(3) have the correct units; c has units of cells/virions and is set to 1. The meaning of this ratio is that each infection is due to the adsorption of one virion to one host cell. We assume all viral strains have the same k because we are interested in variation in burst size and latent period, and adsorption rate is an independent trait. There is loss at rate $d_P P$ due to other mortality (d_P), which is meant to primarily represent grazing. There is also a slow rate of mixing with adjacent waters, $m(P_{\text{in}} - P)$, which causes susceptible hosts from elsewhere (P_{in}) to enter the system at rate m. This term is included to partially stabilize oscillatory dynamics. In equation (2), infected hosts are created through adsorption at rate $\sum_i ckPV_i$, are lost to viral lysis at rate $\sum_i ckV_i^{t-L_i} P^{t-L_i} e^{-(d_P+m)L_i}$, and are lost to other sources of mortality ($d_P I$) or mixing (mI). The product $ckV_i^{t-L_i} P^{t-L_i}$ is the number of hosts infected at time $t - L_i$ by viral strain i, where L_i is the latent period. The term $e^{-(d_P+m)L_i}$ represents the fraction of infected hosts that have not died or been lost to mixing by the end of the latent period. In equation (3), viral strain i (V_i) increases at a rate of $b_i ckV_i^{t-L_i} P^{t-L_i} e^{-(d_P+m)L_i}$, where b_i is the burst size. Free virions are lost as a result of adsorption to new hosts ($kV_i P$), decay at rate d_V, or mixing at rate m. In equation (4), nutrients from elsewhere (N_{in}) enter the system by mixing at rate m and are taken up during phytoplankton growth at rate $q\mu_{\max} PN/(h + N)$, where q is the cellular nutrient content. We have assumed constant nutrient content and Monod-type phytoplankton growth for computational simplicity; the effect of host physiology on infection is implemented via the growth rate–dependent viral production rate (described below). The model does not include recycling of phytoplankton nutrients from lysis or other mortality for simplicity; we have checked to ensure this does not affect the trait evolution results. Parameter values and definitions are given in table 1.

We model the effect of host traits on viral life-history evolution by assuming that the viral burst size b_i is a function of host growth rate $\mu_{\max}$ and the genome size ratio $b_{\max}$:

$$b_i = \min(r(L_i - E), b_{\max}), \quad (5)$$

$$r = \rho_m \times \frac{\mu_{\max} N}{h + N}, \quad (6)$$

$$E = \varepsilon_m \left[\frac{\mu_{\max} N}{h + N}\right]^{-1}. \quad (7)$$

In equation (5), virions are produced intracellularly at a linear rise rate r, beginning after the eclipse period E, which is the time between virion adsorption and the appearance of the first new virions within the host. Burst size b_i is determined by the potential number of virions produced during the latent period L_i, when lysis occurs, or the a priori maximum burst size $b_{\max}$, whichever is smaller. To represent limitation of virion production by host genomic resources, burst size is given the upper limit $b_{\max}$, which is meant to represent the ratio of host genome size : virus genome size. In equation (6), we assume the rise rate r is proportional to host growth rate (with maximum $\rho_m \times \mu_{\max}$). In equation (7), the eclipse period E is inversely proportional to host growth rate (with minimum $e_m/\mu_{\max}$). The functional form of equations (5)–(7) are based on the infection cycle of phage T7 infecting *E. coli* (You et al. 2002). The magnitude of $b_{\max}$, the upper limit on burst size, is varied to test the effect of host genomic resources on viral life-history strategy. The magnitude of $\mu_{\max}$ is varied to test the effect of host growth rate.

To simulate evolution under this model, 100 virus genotypes were initialized at equal low densities, with latent

Table 1: Definition of state variables and parameter values used in the model

State variable/parameter	Description	Units/value
P	Susceptible phytoplankton host density	Cells L^{-1}
V	Free virion density	Virions L^{-1}
I	Infected phytoplankton host density	Cells L^{-1}
N	Dissolved nutrient concentration	μmol L^{-1}
μ_{max}	Maximum growth rate	Varied, .3 to 2 d^{-1}
h	Half-saturation for growth	.02 μmol L^{-1}
k	Adsorption rate	3.6 L^{-1} d^{-1} $cell^{-1}$
c	Infected cells per adsorbed virion	1
d_P	Background phytoplankton mortality	30% of μ_{max}
m	Mixing rate	.1 d^{-1}
d_V	Virion decay rate	Varied, .2 to 1.7 d^{-1}
P_{in}	Susceptible phytoplankton external concentration	10^4 cells L^{-1}
N_{in}	Nutrient external concentration	.5 μmol L^{-1}
Q	Cellular nutrient quota	6.4×10^{-11} μmol $cell^{-1}$
ρ_m	Slope of rise rate vs. host growth rate	Varied, 10–40 × 24 virions $cell^{-1}$
ε_m	Eclipse period scaling factor	3/24
r	Rise rate, $\rho_m \times \frac{\mu_{max} N}{h + N}$	Derived from other parameters
E	Eclipse period, $\varepsilon_m \left[\frac{\mu_{max} N}{h + N}\right]^{-1}$	Derived from other parameters
b_{max}	Maximum possible burst size	Varied, 10–10^6 virions $cell^{-1}$
L_i	Latent period of genotype i	Varied, 2–96 h
b_i	Burst size of genotype i, $\min(r(L_i - E), b_{max})$	Derived from other parameters

Note: For parameters that are varied across simulations, the range of values is given. The value of adsorption rate is typical for phytoplankton viruses (e.g., Cottrell and Suttle 1995; Garry et al. 1998).

periods ranging from 2 to 96 h, and corresponding burst sizes calculated from the above equations. All virus genotypes compete for a single host, and the model was run until one virus genotype competitively excluded all others. Therefore, this is a model of clonal selection among an approximately continuous spectrum of genotypes (Yoshida et al. 2003; Fussmann et al. 2007). This approach does not resolve details of evolution such as mutational distributions or genetic drift, but it allows trait change to be potentially rapid, does not assume steady-state population dynamics, and allows us to ask which strategy will be selected for if sufficient genetic variation exists due to mutation or immigration. In some cases, two adjacent (very similar) genotypes coexisted, and for simplicity we average their traits to a single value in the results. We refer to the selected trait values for latent period and burst size as L_s and b_s, respectively. After running the simulations, we used numerical invasion analysis to confirm that the strategy $L_i = L_s$ is uninvasible by any other genotype. Therefore, the selected trait value L_s is a global evolutionarily stable strategy (Maynard Smith and Price 1973), which is converged upon when sufficient genetic variation is present (our starting conditions).

We use the model to ask how burst size and latent period evolve under different genome size ratios, host growth rates, and other conditions such as mortality rates and nutrient input. The model is eco-evolutionary because evolution of viral traits influences host density, but host density influences viral evolution. This interplay leads to eco-evolutionary feedback (Post and Palkovacs 2009). We chose this approach for several reasons. Previous theory and experiments have shown that optimal latent period of bacteriophage is a function of host density (Wang et al. 1996; Abedon et al. 2003). However, these analyses assume that host density is constant and viruses increase exponentially, but in reality lytic viruses reproduce rapidly and in the process strongly affect host abundance. Therefore, to ask what strategies are likely to evolve under natural conditions, it is sensible to include host-virus population dynamics, while also exploring the role of other factors that will affect host density such as mortality rates and nutrient input. For comparison, we also analyze evolution of viral traits under constant host density. Under constant host density, the viral population will grow without bound. Therefore, we calculate fitness of each viral genotype numerically as the exponential growth rate and find the genotype that maximizes fitness.

The delay differential equations were solved with LSODA in the R package deSolve (Soetaert et al. 2010; supplementary model code, available online; Dryad Digital Repository: http://dx.doi.org/10.5061/dryad.31sm2 [Edwards and Steward 2018]). External inputs to the model are constant (it is a nutrient-limited chemostat/mixed layer model), but the host

and viruses oscillate substantially in abundance (fig. S2). The amplitude of the oscillations is somewhat reduced by the diffusion of susceptible hosts into the system, which aids in computational tractability. Parameter values were chosen to represent a typical phytoplankton-virus system (table 1).

Results: Model of Viral Life-History Evolution

Viral Trait Evolution versus Host Genome Size

To ask how host genomic resources might influence viral trait evolution, we assumed that burst size is constrained by an upper limit b_{max}. This limit could have various causes, but here we will imagine that the total number of nucleotides available for viral genome synthesis is approximately equal to the size of the host genome, and therefore the maximum burst size b_{max} is equal to the host : virus genome size ratio (fig. 1*A*).

Under the assumption of a maximum burst size, the model predicts a nonlinear relationship between burst size and the genome size ratio (fig. 1*C*), as well as between latent period and the genome size ratio (fig. 1*D*). At low size ratios, selection leads to a strategy that maximizes burst size; that is, the selected latent period L_s is the shortest one that will yield the maximal burst size ($b_s = b_{max}$). This means both latent period and burst size increase steeply as the genome size ratio increases, until a threshold is reached at a size ratio of ~1,000 (fig. 1*D*). Above this size ratio, burst size is not maximized and is unrelated to the size ratio. In terms of equation (5), the latent period L_s is short enough that $r(L_s - E) < b_{max}$. The value of other model parameters affects the asymptotic strategy. For example, a lower virion decay rate d_V selects for a greater burst size and longer latent period (fig. 1*D*). A faster virion production rate (ρ_m) also selects for greater asymptotic burst size and latent period, while reducing the latent period needed to reach the maximal burst size (fig. 1*D*). The nutrient input concentration N_{in} and the host mortality rate d_P have modest effects; increased nutrient input slightly reduces latent period, and reduced host mortality slightly increases asymptotic latent period and burst size (fig. S3). We have also varied the other model parameters within a reasonable range (table 1) and found that they have little effect on the model results (results not shown).

These results are consistent with the data showing that burst size and latent period tend to increase with the genome size ratio (fig. 1*A*, 1*B*). In the model, very large genome size ratios lead to a viral life-history strategy that does not exhaust host genomic resources because the fitness cost of the very long latent period is too great. This could explain why latent period seems to be capped at about 50 h (fig. 1*B*), and it could also explain why burst size for small single-stranded viruses, which infect very large hosts, is less correlated with genome size ratio (open triangles and squares in fig. 1*A*).

Viral Trait Evolution versus Host Growth Rate

The model predicts that burst size b_s is largely insensitive to host growth rate, while an increase in host growth rate μ_{max} causes a proportional decline in latent period L_s (fig. 2*D*, 2*E*). In other words, a higher host growth rate allows the same burst size to be achieved with a shorter latent period. Scatter in the relationship between latent period and growth rate can be driven by variation in maximum burst size (b_{max}) or other factors that influence the virion production rate (ρ_m), as also seen in figure 1*C*, 1*D*. These results are consistent with the empirical patterns showing a negative correlation between latent period and host growth rate but no relationship between burst size and growth rate (fig. 2*A*, 2*B*).

To ask how burst size and latent period are expected to covary across viruses, we combined the model results in figure 1*C*, 1*D* (genome size ratio is varied) and figure 2*D*, 2*E* (host growth rate is varied). In other words, we ask how burst size and latent period covary across viruses that have evolved in a realistic range of host environments. Burst size and latent period are positively correlated, but there is substantial variation, in particular because host growth rate alters latent period without changing burst size (fig. 2*F*, filled circles). This pattern is consistent with the positive but weak correlation seen in the data (fig. 2*C*).

Viral Evolution under Constant Host Density

To understand how eco-evolutionary feedback influences viral trait evolution, we held host density constant, that is, it was not regulated by viral lysis. In general, higher host densities select for faster life-history strategies (lower burst size and lower latent period; fig. 4). An additional consequence is that the selected burst size b_s reaches an asymptote at a lower genome size ratio b_{max}. In comparison, variable host density (solid triangles) in the full eco-evolutionary model selects for relatively slower life-history strategies. Under the highest genome size ratios, the full model yields a burst size and latent period somewhat larger than are selected for under a constant host density of 10^6 cells L^{-1} (fig. 4). Compared to an extremely high host density of 10^{10} L^{-1}, the full model achieves a burst size that is ~30 times greater, as well as a much greater range of burst sizes. These results indicate that trait evolution in the eco-evolutionary model depends on the fact that host densities are regulated by the virus (without the virus, the host reaches $\sim 2 \times 10^9$ L^{-1}). Low host density, in turn, selects for longer latent period, because it is less advantageous for the virus to leave the host cell before resources are exhausted. In nature, grazing and resource competition would also act to reduce host density and thus influence trait

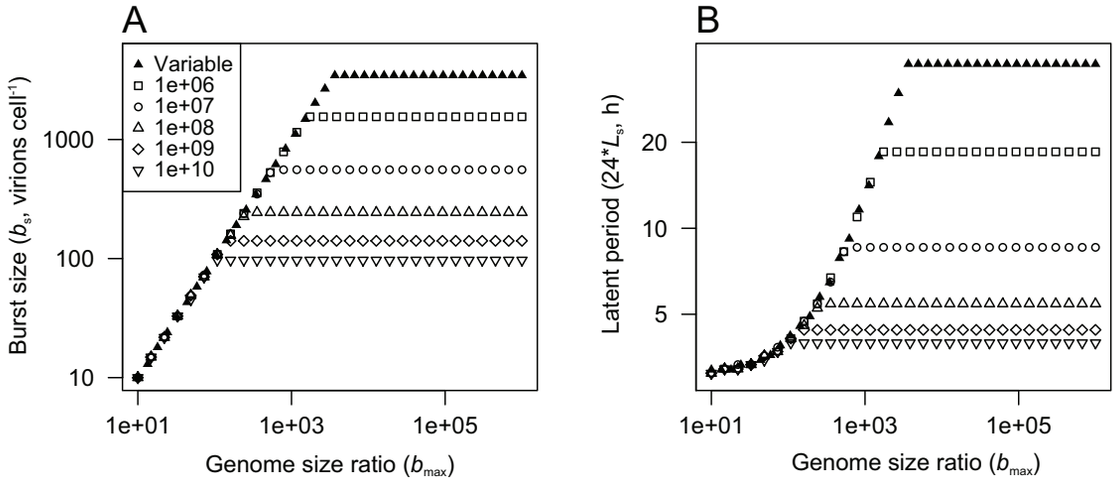

Figure 4: Modeled trait evolution under constant host density. *A*, Burst size (b_s) versus genome size ratio (b_{max}). *B*, Latent period (L_s) versus genome size ratio (b_{max}). The trait values plotted are the optimal (highest fitness) strategies at each combination of host density and genome size ratio. Fitness is calculated numerically as the long-term exponential growth rate of the viral genotype at the appropriate host density. The symbols show host densities from 10^6 to 10^{10} cells L^{-1}. Also included are the model results when host density is not held constant, that is, the full eco-evolutionary model (filled triangles, which correspond to the filled triangles in fig. 1*C*, 1*D*). No viral genotype could persist when host density $= 10^6$ and genome size ratio $< 10^2$. The values of the model parameters are as follows: maximum growth rate $\mu_{max} = 1$, viral decay rate $d_V = 0.2$, and virion production rate constant $r_m = 100$; other parameters are assigned the values in table 1.

evolution. Under constant host density, the effect of host growth rate μ_{max} on viral trait evolution is qualitatively similar to the results in the full eco-evolutionary model (results not shown).

Discussion

We find that traits of the phytoplankton host (genome size and growth rate), in combination with virus genome size, can collectively explain ~40%–50% of variation in burst size and latent period across phytoplankton viruses characterized thus far. A model of latent period evolution, parameterized with realistic values, produces patterns similar to the empirical results. This congruence between data and model predictions lends support to the hypothesized underlying mechanisms. Our interpretation of these results is that phytoplankton cells are a sparse resource in a world that is relatively hazardous for free virions. Low host density selects for latent periods that exhaust host resources before lysis, at least for viruses that are not extremely small compared to their host. This results in a correlation between total nucleotide output and host genome size, or between burst size and the host : virus genome size ratio, as found previously for 15 host-virus pairs (Brown et al. 2006). In addition, latent period is jointly influenced by the genome size ratio and the host growth rate because the physiology of more rapid host growth allows for more rapid virion production. When the genome size ratio is very large (greater than ~1,000), it may be that latent period would have to be several days long in order to exhaust host resources, which increases the likelihood of host mortality during infection. Under these conditions, other factors may determine the evolution of latent period, such as mortality rates of the host and free virions. In total, our results argue that a trait-based approach to viral ecology is promising, and important aspects of community dynamics and evolution may be predictable from a relatively simple set of underlying principles.

The patterns documented here across viral strains can be compared with short-term experiments on a single strain, where host growth is manipulated and virus replication is characterized. Experiments with *E. coli* typically show that increased host growth rate decreases latent period and increases burst size (You et al. 2002). In an experiment with *Synechococcus*, an increase in growth due to stirring did not alter latent period (Wilson et al. 1996), while experiments with *Micromonas* and *Phaeocystis* found that both nitrogen- and phosphorus-limited growth increased latent period and reduced burst size (Maat and Brussaard 2016). These plasticity-driven correlations between burst size and host growth rate differ from our empirical and model results (fig. 2). In this context, it is important to note that short-term plastic responses of a strain may differ from the evolved strategies that vary across strains and hosts. Indeed, in our model the immediate effect of faster host growth is to increase the rate of viral production, which will lead to a greater burst size for a particular latent period. However, over the long term the optimal genotype is one

that reduces the latent period while maintaining the same burst size.

Our compilation is relevant to some additional questions not addressed by our model, which focused on the evolution of burst size and latent period. Viruses of phytoplankton vary greatly in size, and the maintenance of this size variation remains to be explained. All else being equal, larger virions should take longer to synthesize/assemble, and if host resources are limiting, then fewer virions can be produced. Both considerations should reduce burst size for larger viruses, but this is only modestly evident in the data (fig. 3*A*). A similar pattern is found when (burst size)/(latent period) is used to approximate the rate of virion production (fig. S1*C*). There is evidence that larger viral genome size allows for better control of host metabolism, which could increase the rate of viral production and/or the contribution of de novo nucleotide synthesis (Lindell et al. 2005; Hurwitz et al. 2013). Modeling a general mechanistic relationship between genome size and viral replication will require a complex model of host-viral metabolism and its evolution (Bragg and Chisholm 2008; Birch et al. 2012).

The patterns in our compilation are most evident for dsDNA viruses, which have been studied in much greater detail than other types. It is possible that single-stranded viruses are under distinct selective pressures as a consequence of their very small size or different type of interaction with host systems of transcription/translation/replication. In addition, at this point, single-stranded viruses of phytoplankton have been isolated primarily from *Chaetoceros* spp. (e.g., Nagasaki et al. 2005; Tomaru et al. 2008; Kimura and Tomaru 2015). The authors of those studies further note that burst size is hard to define, because it appears that new viral particles are released prior to lysis. Therefore, a somewhat different mode of infection may be part of the reason the strains show different patterns in our analyses. An additional factor that could add noise or bias to the data is the fact that viral strains maintained in culture could evolve in response to propagation. During propagation, viruses are periodically exposed to relatively high host density, which could select for a shorter latent period.

The results of this study can contribute to models of virus-microbe interactions, community structure, and ecosystem consequences. Recent models have explored how viruses can promote host diversity (Thingstad et al. 2014), how hosts and viruses with overlapping host ranges can coexist (Jover et al. 2013), and how viruses alter the dynamics of standard ecosystem models (Weitz et al. 2015), among other topics. The relationships between virus and host traits described here could be used to constrain model parameters, allowing host and virus community structure to self-organize across environmental gradients (Follows and Dutkiewicz 2011). Cell size is a master trait that influences many aspects of plankton ecology (Finkel et al. 2009; Edwards et al. 2012), and size has been used to structure trait-based models via allometric scaling relationships (Follows and Dutkiewicz 2011). Genome size is well correlated with cell size in phytoplankton and other organisms (Veldhuis et al. 1997), and therefore the results of the current study could be used to derive scaling relationships and incorporate viral dynamics into size-structured models of plankton ecosystems. Successful development of virus community models will also require considerable empirical progress on how host range and host resistance coevolve and how infection network structure is related to both viral traits (burst size, adsorption rate, etc.) and host traits (resistance and its physiological costs).

Acknowledgments

We thank Spencer Hall, David Talmy, Sergio Vallina, and Alice Winn for comments on the manuscript. This work is funded by National Science Foundation Division of Ocean Sciences grant 1559356.

Literature Cited

Abedon, S. T., P. Hyman, and C. Thomas. 2003. Experimental examination of bacteriophage latent-period evolution as a response to bacterial availability. Applied and Environmental Microbiology 69:7499–7506.

Bartón, K. 2016. MuMIn: multi-model inference. R package. Version 1.15.6. https://CRAN.R-project.org/package=MuMIn.

Bates, D., M. Maechler, B. Bolker, and S. Walker. 2015. Fitting linear mixed-effects models using lme4. Journal of Statistical Software 67: 1–48.

Birch, E. W., N. A. Ruggero, and M. W. Covert. 2012. Determining host metabolic limitations on viral replication via integrated modeling and experimental perturbation. PLoS Computational Biology 8:e1002746.

Bonachela, J. A., and S. A. Levin. 2014. Evolutionary comparison between viral lysis rate and latent period. Journal of Theoretical Biology 345:32–42.

Bragg, J. G., and S. W. Chisholm. 2008. Modeling the fitness consequences of a cyanophage-encoded photosynthesis gene. PLoS ONE 3:1–9.

Breitbart, M. 2012. Marine viruses: truth or dare. Annual Review of Marine Science 4:425–448.

Brown, C. M., D. A. Campbell, and J. E. Lawrence. 2007. Resource dynamics during infection of *Micromonas pusilla* by virus MpV-Sp1. Environmental Microbiology 9:2720–2727.

Brown, C. M., J. E. Lawrence, and D. A. Campbell. 2006. Are phytoplankton population density maxima predictable through analysis of host and viral genomic DNA content? Journal of the Marine Biological Association of the UK 86:491.

Brussaard, C. P. D. 2004. Viral control of phytoplankton populations: a review. Journal of Eukaryotic Microbiology 51:125–138.

Cottrell, M. T., and C. A. Suttle. 1995. Dynamics of a lytic virus infecting the photosynthetic marine picoflagellate *Micromonas pusilla*. Limnology and Oceanography 40:730–739.

Daines, S. J., J. R. Clark, and T. M. Lenton. 2014. Multiple environmental controls on phytoplankton growth strategies determine adaptive responses of the N : P ratio. Ecology Letters 17:414–425.

Edwards, K. F., and G. F. Steward. 2018. Data from: Host traits drive viral life histories across phytoplankton viruses. American Naturalist, Dryad Digital Repository, http://dx.doi.org/10.5061/dryad.31sm2.

Edwards, K. F., M. K. Thomas, C. A. Klausmeier, and E. Litchman. 2012. Allometric scaling and taxonomic variation in nutrient utilization traits and maximum growth rate of phytoplankton. Limnology and Oceanography 57:554–566.

Falkowski, P. G., M. E. Katz, A. H. Knoll, A. Quigg, J. A. Raven, O. Schofield, and F. J. R. Taylor. 2004. The evolution of modern eukaryotic phytoplankton. Science 305:354–360.

Finkel, Z. V., J. Beardall, K. J. Flynn, A. Quigg, T. A. V. Rees, and J. A. Raven. 2009. Phytoplankton in a changing world: cell size and elemental stoichiometry. Journal of Plankton Research 32:119–137.

Fischer, M. G. 2016. Giant viruses come of age. Current Opinions in Microbiology 31:50–57.

Follows, M. J., and S. Dutkiewicz. 2011. Modeling diverse communities of marine microbes. Annual Review of Marine Science 3:427–451.

Fussmann, G. F., M. Loreau, and P. A. Abrams. 2007. Eco-evolutionary dynamics of communities and ecosystems. Functional Ecology 21: 465–477.

Garry, R. T., P. Hearing, and E. M. Cosper. 1998. Characterization of a lytic virus infectious to the bloom-forming microalga *Aureococcus anophagefferens* (Pelagophyceae). Journal of Phycology 621:616–621.

Gudelj, I., J. S. Weitz, T. Ferenci, M. Claire Horner-Devine, C. J. Marx, J. R. Meyer, and S. E. Forde. 2010. An integrative approach to understanding microbial diversity: from intracellular mechanisms to community structure. Ecology Letters 13:1073–1084.

Hurwitz, B. L., S. J. Hallam, and M. B. Sullivan. 2013. Metabolic reprogramming by viruses in the sunlit and dark ocean. Genome Biology 14:R123.

Jover, L. F., M. H. Cortez, and J. S. Weitz. 2013. Mechanisms of multi-strain coexistence in host-phage systems with nested infection networks. Journal of Theoretical Biology 332:65–77.

Kimura, K., and Y. Tomaru. 2015. Discovery of two novel viruses expands the diversity of single-stranded DNA and single-stranded RNA viruses infecting a cosmopolitan marine diatom. Applied and Environmental Microbiology 81:1120–1131.

Koonin, E. V., and V. V. Dolja. 2013. A virocentric perspective on the evolution of life. Current Opinion in Virology 3:546–557.

Kuznetsova, A., P. B. Brockhoff, and R. H. B. Christensen. 2016. lmerTest: tests in linear mixed effects models. R package. Version 2.0-32. https://cran.r-project.org/web/packages/lmerTest/index.html.

Lang, A. S., M. L. Rise, A. I. Culley, and G. Steward. 2009. RNA viruses in the sea. FEMS Microbiology Reviews 33:295–323.

Levin, B., F. Stewart, and L. Chao. 1977. Resource-limited growth, competition, and predation: a model and experimental studies with bacteria and bacteriophage. American Naturalist 111:3–24.

Lindell, D., J. D. Jaffe, Z. I. Johnson, G. M. Church, and S. W. Chisholm. 2005. Photosynthesis genes in marine viruses yield proteins during host infection. Nature 438:86–89.

Litchman, E., and C. A. Klausmeier. 2008. Trait-based community ecology of phytoplankton. Annual Review of Ecology, Evolution, and Systematics 39:615–639.

Maat, D. S., and C. P. D. Brussaard. 2016. Both phosphorus- and nitrogen limitation constrain viral proliferation in marine phytoplankton. Aquatic Microbial Ecology 77:87–97.

Maynard Smith, J., and G. F. Price. 1973. The logic of animal conflict. Nature 246:15–18.

Nagasaki, K., Y. Tomaru, Y. Takao, K. Nishida, Y. Shirai, H. Suzuki, and T. Nagumo. 2005. Previously unknown virus infects marine diatom. Applied and Environmental Microbiology 71:3528–3535.

Post, D. M., and E. P. Palkovacs. 2009. Eco-evolutionary feedbacks in community and ecosystem ecology: interactions between the ecological theatre and the evolutionary play. Philosophical Transactions of the Royal Society B 364:1629–1640.

Rosario, K., S. Duffy, and M. Breitbart. 2012. A field guide to eukaryotic circular single-stranded DNA viruses: insights gained from metagenomics. Archives of Virology 157:1851–1871.

Soetaert, K., T. Petzoldt, and R. W. Setzer. 2010. Solving differential equations in R: package deSolve. Journal of Statistical Software 33:1–25.

Steward, G. F., A. I. Culley, and E. M. Wood-Charlson. 2013. Marine viruses. Pages 127–144 *in* S. A. Levin, ed. Encyclopedia of biodiversity. 2nd ed. Academic Press, San Diego, CA.

Suttle, C. A. 2007. Marine viruses—major players in the global ecosystem. Nature Reviews Microbiology 5:801–812.

Thingstad, T. F., S. Våge, J. E. Storesund, R.-A. Sandaa, and J. Giske. 2014. A theoretical analysis of how strain-specific viruses can control microbial species diversity. Proceedings of the National Academy of Sciences of the USA 111:7813–7818.

Thomas, R., N. Grimsley, M.-L. Escande, L. Subirana, E. Derelle, and H. Moreau. 2011. Acquisition and maintenance of resistance to viruses in eukaryotic phytoplankton populations. Environmental Microbiology 13:1412–1420.

Thompson, L. R., Q. Zeng, L. Kelly, K. H. Huang, A. U. Singer, J. Stubbe, and S. W. Chisholm. 2011. Phage auxiliary metabolic genes and the redirection of cyanobacterial host carbon metabolism. Proceedings of the National Academy of Sciences of the USA 108:E757–E764.

Tomaru, Y., Y. Shirai, H. Suzuki, T. Nagumo, and K. Nagasaki. 2008. Isolation and characterization of a new single-stranded DNA virus infecting the cosmopolitan marine diatom *Chaetoceros debilis*. Aquatic Microbial Ecology 50:103–112.

Tummers, B. 2006. DataThief III. http://datathief.org/.

Van Etten, J. L., D. E. Burbank, J. Joshi, and R. H. Meints. 1984. DNA synthesis in a *Chlorella*-like alga following infection with the virus PBCV-1. Virology 134:443–449.

Veldhuis, M. J. W., T. L. Cucci, and M. E. Sieracki. 1997. Cellular DNA content of marine phytoplankton using two new fluorochromes: taxonomic and ecological implications. Journal of Phycology 33:527–541.

Villarreal, L. P., and G. Witzany. 2010. Viruses are essential agents within the roots and stem of the tree of life. Journal of Theoretical Biology 262:698–710.

Wang, I.-N., D. E. Dykhuizen, and L. B. Slobodkin. 1996. The evolution of phage lysis timing. Evolutionary Ecology 10:545–558.

Weitz, J. S., C. A. Stock, S. W. Wilhelm, L. Bourouiba, M. L. Coleman, A. Buchan, M. J. Follows, et al. 2015. A multitrophic model to quantify the effects of marine viruses on microbial food webs and ecosystem processes. ISME Journal 9:1352–1364.

Westoby, M., and I. J. Wright. 2006. Land-plant ecology on the basis of functional traits. Trends in Ecology and Evolution 21:261–268.

Wikner, J., J. J. Vallino, G. F. Steward, D. C. Smith, and F. Azam. 1993. Nucleic acids from the host bacterium as a major source of nucleotides for 3 marine bacteriophages. FEMS Microbiology Ecology 12:237–248.

Wilson, W. H., N. G. Carr, and N. H. Mann. 1996. The effect of phosphate status on the kinetics of cyanophage infection in the

oceanic cyanobacterium *Synechococcus* sp. WH7803. Journal of Phycology 32:506–516.

Yoshida, T., L. E. Jones, S. P. Ellner, G. F. Fussmann, and N. G. Hairston Jr. 2003. Rapid evolution drives ecological dynamics in a predator-prey system. Nature 424:303–306.

You, L., P. F. Suthers, and J. Yin. 2002. Effects of *Escherichia coli* physiology on growth of phage T7 in vivo and in silico. Journal of Bacteriology 184:1497–1500.

References Cited Only in the Supplementary Material

Adolph, K., and R. Haselkorn. 1972. Photosynthesis and the development of blue-green algal virus N-1. Virology 47:370–374.

Akcaalan, R., F. M. Young, J. S. Metcalf, L. F. Morrison, M. Albay, and G. A. Codd. 2006. Microcystin analysis in single filaments of *Planktothrix* spp. in laboratory cultures and environmental blooms. Water Research 40:1583–1590.

Arora, M., A. C. Anil, F. Leliaert, J. Delany, and E. Mesbahi. 2013. *Tetraselmis indica* (Chlorodendrophyceae, Chlorophyta), a new species isolated from salt pans in Goa, India. European Journal of Phycology 48:61–78.

Bancroft, I., and R. Smith. 1989. Restriction mapping of genomic DNA from five cyanophages infecting the heterocystous cyanobacteria Nostoc and Anabaena. New Phytologist 113:161–166.

Baudoux, A. C., and C. P. D. Brussaard. 2005. Characterization of different viruses infecting the marine harmful algal bloom species *Phaeocystis globosa*. Virology 341:80–90.

Blanc, G., G. Duncan, I. Agarkova, M. Borodovsky, J. Gurnon, A. Kuo, E. Lindquist, et al. 2010. The *Chlorella variabilis* NC64A genome reveals adaptation to photosymbiosis, coevolution with viruses, and cryptic sex. Plant Cell 22:2943–2955.

Boenigk, J., C. Matz, K. Jürgens, and H. Arndt. 2001. The influence of preculture conditions and food quality on the ingestion and digestion process of three species of heterotrophic nanoflagellates. Microbial Ecology 42:168–176.

Bosak, S., M. G. Udovič, and D. Sarno. 2015. Morphological study of *Chaetoceros wighamii* Brightwell (Chaetocerotaceae, Bacillariophyta) from Lake Vrana, Croatia. Acta Botanica Croatica 74:233–244.

Brown, C. M., and K. D. Bidle. 2014. Attenuation of virus production at high multiplicities of infection in *Aureococcus anophagefferens*. Virology 466/467:71–81.

Brussaard, C. P. D., A. A. M. Noordeloos, R. A. Sandaa, M. Heldal, and G. Bratbak. 2004. Discovery of a dsRNA virus infecting the marine photosynthetic protist *Micromonas pusilla*. Virology 319:280–291.

Campbell, L., H. Nolla, and D. Vaulot. 1994. The importance of *Prochlorococcus* to community structure in the central North Pacific Ocean. Limnology and Oceanography 39:954–961.

Castberg, T., R. Thyrhaug, A. Larsen, R. A. Sandaa, M. Heldal, J. L. Van Etten, and G. Bratbak. 2002. Isolation and characterization of a virus that infects *Emiliania huxleyi* (Haptophyta). Journal of Phycology 38:767–774.

Chénard, C. 2014. Genomic characterization of viruses infecting freshwater polar cyanobacteria. PhD diss. University of British Columbia, Vancouver.

Connolly, J. A., M. J. Oliver, J. M. Beaulieu, C. A. Knight, L. Tomanek, and M. A. Moline. 2008. Correlated evolution of genome size and cell volume in diatoms (Bacillariophyceae). Journal of Phycology 44:124–131.

Cottrell, M. T., and C. A. Suttle. 1991. Wide-spread occurrence and clonal variation in viruses which cause lysis of a cosmopolitan, eukaryotic marine phytoplankter, *Micromonas pusilla*. Marine Ecology Progress Series 78:1–9.

Derelle, E., C. Ferraz, M. L. Escande, S. Eychenié, R. Cooke, G. Piganeau, Y. Desdevises, L. Bellec, H. Moreau, and N. Grimsley. 2008. Life-cycle and genome of OtV5, a large DNA virus of the pelagic marine unicellular green alga *Ostreococcus tauri*. PLoS ONE 3:e2250.

Dufresne, A., M. Ostrowski, D. J. Scanlan, L. Garczarek, S. Mazard, B. Palenik, I. T. Paulsen, et al. 2008. Unraveling the genomic mosaic of a ubiquitous genus of marine cyanobacteria. Genome Biology 9:R90.

Durand, M. D., R. E. Green, H. M. Sosik, and R. J. Olson. 2002. Diel variations in optical properties of *Micromonas pusilla* (Prasinophyceae). Journal of Phycology 38:1132–1142.

Dvořák, P., D. A. Casamatta, A. Poulíčková, P. Hašler, V. Ondřej, and R. Sanges. 2014. *Synechococcus*: 3 billion years of global dominance. Molecular Ecology 23:5538–5551.

Edwards, K. F., M. K. Thomas, C. A. Klausmeier, and E. Litchman. 2015. Light and growth in marine phytoplankton: allometric, taxonomic, and environmental variation. Limnology and Oceanography 60:540–552.

Eissler, Y., K. Wang, F. Chen, K. Eric Wommack, and D. Wayne Coats. 2009. Ultrastructural characterization of the lytic cycle of an intranuclear virus infecting the diatom *Chaetoceros* cf. *wighamii* (bacillariophyceae) from Chesapeake Bay, USA. Journal of Phycology 45:787–797.

Frois-Moniz, K. 2014. Host/virus interactions in the marine cyanobacterium *Prochlorococcus*. PhD diss. Massachusetts Institute of Technology, Cambridge, MA.

Gallot-Lavallé, L., A. Pagarete, M. Legendre, S. Santini, R. Sandaa, H. Himmelbauer, H. Ogata, G. Bratbak, and J. Claverie. 2015. The 474-kilobase-pair complete genome sequence of CeV-01B, a virus infecting *Haptolina* (*Chrysochromulina*) *ericina* emerging subclade of the Megaviridae family with smaller genomes and particles than the originally described giant Mimiviridae. Genome Announcements 3:1–2.

Gao, E.-B., J.-F. Gui, and Q.-Y. Zhang. 2012. A novel cyanophage with a cyanobacterial nonbleaching protein A gene in the genome. Journal of Virology 86:236–245.

Gao, E. B., X. P. Yuan, R. H. Li, and Q. Y. Zhang. 2009. Isolation of a novel cyanophage infectious to the filamentous cyanobacterium *Planktothrix agardhii* (Cyanophyceae) from Lake Donghu, China. Aquatic Microbial Ecology 54:163–170.

Gobler, C. J., D. L. Berry, S. T. Dyhrman, S. W. Wilhelm, A. Salamov, A. V Lobanov, Y. Zhang, et al. 2011. Niche of harmful alga *Aureococcus anophagefferens* revealed through ecogenomics. Proceedings of the National Academy of Sciences of the USA 108:4352–4357.

Goldstein, D. A., I. J. Bendet, M. A. Lauffer, and K. M. Smith. 1967. Some biological and physicochemical properties of blue-green algal virus Lpp-1. Virology 32:601–613.

Gromov, B. 1983. Cyanophages. Annales de l'Institut Pasteur Microbiologie 134B:43–59.

Hahn, A., M. Stevanovic, O. Mirus, and E. Schleiff. 2012. The TolC-like protein HgdD of the cyanobacterium *Anabaena* sp. PCC 7120 is involved in secondary metabolite export and antibiotic resistance. Journal of Biological Chemistry 287:41126–41138.

Hansen, P. E. R. J., T. O. M. Fenchel, and P. Juel Hansen. 2006. The bloom-forming ciliate *Mesodinium rubrum* harbours a single permanent endosymbiont. Marine Biology Research 2:169–177.

Harrison, P. J., H. L. Conway, and R. C. Dugdale. 1976. Marine diatoms grown in chemostats under silicate or ammonium limita-

tion. I. Cellular chemical composition and steady state growth kinetics of *Skeletonema costatum*. Marine Biology 35:177–186.

Harrison, P. J., A. Zingone, M. J. Mickelson, S. Lehtinen, N. Ramaiah, A. C. Kraberg, J. Sun, A. McQuatters-Gollop, and H. H. Jakobsen. 2015. Cell volumes of marine phytoplankton from globally distributed coastal data sets. Estuarine, Coastal and Shelf Science 162:130–142.

Heldal, M., D. J. Scanlan, S. Norland, F. Thingstad, and N. H. Mann. 2003. Elemental composition of single cells of various strains of marine *Prochlorococcus* and *Synechococcus* using X-ray microanalysis. Limnology and Oceanography 48:1732–1743.

Herdman, M., M. Janvier, R. Rippka, and R. Y. Stanier. 1979. Genome size of cyanobacteria. Journal of General Microbiology 111:73–85.

Holtman, C. K., Y. Chen, P. Sandoval, A. Gonzales, M. S. Nalty, T. L. Thomas, P. Youderian, and S. S. Golden. 2005. High-throughput functional analysis of the *Synechococcus elongatus* PCC 7942 genome. DNA Research 12:103–115.

Hu, B., G. Yang, W. Zhao, Y. Zhang, and J. Zhao. 2007. MreB is important for cell shape but not for chromosome segregation of the filamentous cyanobacterium *Anabaena* sp. PCC 7120. Molecular Microbiology 63:1640–1652.

Jacobsen, A., G. Bratbak, and M. Heldal. 1996. Isolation and characterization of a virus infecting *Phaeocystis pouchetii* (Prymnesiophyceae). Journal of Phycology 32:923–927.

Jacquet, S., and G. Bratbak. 2003. Effects of ultraviolet radiation on marine virus-phytoplankton interactions. FEMS Microbiology Ecology 44:279–289.

Jahnke, J. 1989. The light and temperature dependence of growth rate and elemental composition of *Phaeocystis globosa* Scherffel and *P. pouchetii* (Har.) Lagerh. in batch cultures. Netherlands Journal of Sea Research 23:15–21.

Jia, Y., J. Shan, A. Millard, M. R. J. Clokie, and N. H. Mann. 2010. Light-dependent adsorption of photosynthetic cyanophages to *Synechococcus* sp. WH7803. FEMS Microbiology Letters 310:120–126.

Johannessen, T. V., G. Bratbak, A. Larsen, H. Ogata, E. S. Egge, B. Edvardsen, W. Eikrem, and R. A. Sandaa. 2015. Characterisation of three novel giant viruses reveals huge diversity among viruses infecting Prymnesiales (Haptophyta). Virology 476:180–188.

Kim, J., C. H. Kim, Y. Takano, I. K. Jang, S. W. Kim, and T. J. Choi. 2012. Isolation and physiological characterization of a new algicidal virus infecting the harmful dinoflagellate *Heterocapsa pygmaea*. Plant Pathology Journal 28:433–438.

Kim, J., C. H. Kim, S. Youn, and T. Choi. 2015. Isolation and physiological characterization of a novel algicidal virus infecting the marine diatom *Skeletonema costatum*. Plant Pathology Journal 31: 186–191.

Kim, J., S.-H. Yoon, and T.-J. Choi. 2015. Isolation and physiological characterization of a novel virus infecting *Stephanopyxis palmeriana* (Bacillariophyta). Algae 30:81–87.

Kimura, K., and Y. Tomaru. 2013. Isolation and characterization of a single-stranded DNA virus infecting the marine diatom *Chaetoceros* sp. strain SS628-11 isolated from western Japan. PLoS ONE 8:e82013.

Knisely, K., and W. Geller. 1986. Selective feeding of four zooplankton species on natural lake phytoplankton. Oecologia 69:86–94.

Lajeunesse, T. C., R. A. Andersen, and D. W. Galbraith. 2005. *Symbiodinium* (Pyrrophyta) genomes sizes (DNA content) are smallest among dinoflagellates. Journal of Phycology 41:880–886.

Leach, J., K. Lee, R. Benson, and E. Martin. 1980. Ultrastructure of the infection cycle of cyanophage SM-2 in *Synechococcus elongatus* (Cyanophyceae). Journal of Phycology 16:307–310.

Li, Y., Z. Lu, L. Sun, S. Ropp, G. F. Kutish, D. L. Rock, and J. L. Van Etten. 1997. Analysis of 74 kb of DNA located at the right end of the 330-kb chlorella virus PBCV-1 genome. Virology 237:360–377.

Liu, X., S. Kong, M. Shi, L. Fu, Y. Gao, and C. An. 2008. Genomic analysis of freshwater cyanophage Pf-WMP3 infecting cyanobacterium *Phormidium foveolarum*: the conserved elements for a phage. Microbial Ecology 56:671–680.

Liu, X., M. Shi, S. Kong, Y. Gao, and C. An. 2007. Cyanophage Pf-WMP4, a T7-like phage infecting the freshwater cyanobacterium *Phormidium foveolarum*: complete genome sequence and DNA translocation. Virology 366:28–39.

Long, B., G. Jones, and P. Orr. 2001. Cellular microcystin content in N-limited *Microcystis aeruginosa* can be predicted from growth rate. Microbiology 67:278–283.

Mackenzie, J. J., and R. Haselkorn. 1972*a*. An electron microscope study of infection by the blue-green algal virus SM-1. Virology 49:505–516.

———. 1972*b*. Physical properties of blue-green algal virus SM-1 and its DNA. Virology 49:497–504.

Mann, N. H., M. R. J. Clokie, A. Millard, A. Cook, W. H. Wilson, P. J. Wheatley, A. Letarov, and H. M. Krisch. 2005. The genome of S-PM2, a "photosynthetic" T4-type bacteriophage that infects marine *Synechococcus* strains. Journal of Bacteriology 187:3188–3200.

McAuley, P. J. 1987. Nitrogen limitation and amino-acid metabolism of *Chlorella* symbiotic with green hydra. Planta 171:532–538.

McEwan, M., R. Humayun, C. H. Slamovits, and P. J. Keeling. 2008. Nuclear genome sequence survey of the dinoflagellate *Heterocapsa triquetra*. Journal of Eukaryotic Microbiology 55:530–535.

Mirza, S. F., M. A. Staniewski, C. M. Short, A. M. Long, Y. V. Chaban, and S. M. Short. 2015. Isolation and characterization of a virus infecting the freshwater algae *Chrysochromulina parva*. Virology 486:105–115.

Moniruzzaman, M., G. R. LeCleir, C. M. Brown, C. J. Gobler, K. D. Bidle, W. H. Wilson, and S. W. Wilhelm. 2014. Genome of brown tide virus (AaV), the little giant of the Megaviridae, elucidates NCLDV genome expansion and host-virus coevolution. Virology 466/467:60–70.

Montealegre, R. J., J. Verreth, K. Steenbergen, J. Moed, and M. Machiels. 1995. A dynamic simulation model for the blooming of *Oscillatoria agardhii* in a monomictic lake. Ecological Modelling 78:17–24.

Morel, A., Y.-H. Ahn, F. Partensky, D. Vaulot, and H. Claustre. 1993. *Prochlorococcus* and *Synechococcus*: a comparative study of their optical properties in relation to their size and pigmentation. Journal of Marine Research 51:617–649.

Nagasaki, K., J.-J. Kim, Y. Tomaru, Y. Takao, and S. Nagai. 2009. Isolation and characterization of a novel virus infecting *Teleaulax amphioxeia* (Cryptophyceae). Plankton and Benthos Research 4:122–124.

Nagasaki, K., Y. Shirai, Y. Takao, H. Mizumoto, K. Nishida, and Y. Tomaru. 2005. Comparison of genome sequences of single-stranded RNA viruses infecting the bivalve-killing dinoflagellate *Heterocapsa circularisquama*. Applied and Environmental Microbiology 71:8888–8894.

Nagasaki, K., K. Tarutani, and M. Yamaguchi. 1999. Growth characteristics of *Heterosigma akashiwo* virus and its possible use as a microbial agent for red tide control. Applied and Environmental Microbiology 65:898–902.

Nagasaki, K., Y. Tomaru, N. Katanozaka, Y. Shirai, K. Nishida, S. Itakura, and M. Yamaguchi. 2004. Isolation and characterization

of a novel single-stranded RNA virus infecting the bloom-forming diatom *Rhizosolenia setigera*. Applied and Environmental Microbiology 70:704–711.

Nagasaki, K., Y. Tomaru, K. Tarutani, S. Yamanaka, H. Tanabe, and N. Katanozaka. 2003. Growth characteristics and intraspecies host specificity of a large virus infecting the dinoflagellate *Heterocapsa circularisquama*. Applied and Environmental Microbiology 69:2580–2586.

Ou, T., S. Li, X. Liao, and Q. Zhang. 2013. Cultivation and characterization of the MaMV-DC cyanophage that infects bloom-forming cyanobacterium *Microcystis aeruginosa*. Virologica Sinica 28:266–271.

Ou, T., X. Y. Liao, X. C. Gao, X. D. Xu, and Q. Y. Zhang. 2015. Unraveling the genome structure of cyanobacterial podovirus A-4L with long direct terminal repeats. Virus Research 203:4–9.

Padan, E., D. Ginzburg, and M. Shilo. 1970. The reproductive cycle of cyanophage LPPl-G in *Plectonema boryanum* and its dependence on photosynthetic and respiratory systems. Virology 40:514–521.

Pagarete, A., T. Grébert, O. Stepanova, R.-A. Sandaa, and G. Bratbak. 2015. Tsv-N1: a novel DNA algal virus that infects *Tetraselmis striata*. Viruses 7:3937–3953.

Palinska, K., B. Deventer, K. Hariri, and M. Lotocka. 2011. A taxonomic study on Phormidium-group (cyanobacteria) based on morphology, pigments, RAPD molecular markers and RFLP analysis of the 16S rRNA gene fragment. Fottea 11:41–55.

Raytcheva, D. A., C. Haase-Pettingell, J. M. Piret, and J. A. King. 2011. Intracellular assembly of cyanophage Syn5 proceeds through a scaffold-containing procapsid. Journal of Virology 85:2406–2415.

Read, B. A., J. Kegel, M. J. Klute, A. Kuo, S. C. Lefebvre, F. Maumus, C. Mayer, et al. 2013. Pan genome of the phytoplankton *Emiliania* underpins its global distribution. Nature 499:209–213.

Reynolds, C. S., and E. G. Bellinger. 1992. Patterns of abundance and dominance of the phytoplankton of Rostherne Mere, England: evidence from an 18-year data set. Aquatic Sciences 54:10–36.

Riegman, R., and W. Stolte. 2000. Nutrient uptake and alkaline phosphatase (EC 3:1:3:1) activity of *Emiliania huxleyi* (Prymnesiophyceae) during growth under N and P limitation in continuous cultures. Journal of Phycology 36:87–96.

Rocap, G., F. W. Larimer, J. Lamerdin, S. Malfatti, P. Chain, N. A. Ahlgren, A. Arellano, et al. 2003. Genome divergence in two *Prochlorococcus* ecotypes reflects oceanic niche differentiation. Nature 424:1042–1047.

Sabehi, G., L. Shaulov, D. H. Silver, I. Yanai, A. Harel, and D. Lindell. 2012. A novel lineage of myoviruses infecting cyanobacteria is widespread in the oceans. Proceedings of the National Academy of Sciences of the USA 109:2037–2042.

Safferman, R., T. Diener, P. Desjardins, and M. Morris. 1972. Isolation and characterization of AS-1, a phycovirus infecting the blue-green algae, *Anacystis nidulans* and *Synechococcus cedrorum*. Virology 47:105–113.

Sandaa, R. A., M. Heldal, T. Castberg, R. Thyrhaug, and G. Bratbak. 2001. Isolation and characterization of two viruses with large genome size infecting *Chrysochromulina ericina* (Prymnesiophyceae) and *Pyramimonas orientalis* (Prasinophyceae). Virology 290:272–280.

Savichtcheva, O., D. Debroas, R. Kurmayer, C. Villar, J. P. Jenny, F. Arnaud, M. E. Perga, and I. Domaizon. 2011. Quantitative PCR enumeration of total/toxic *Planktothrix rubescens* and total cyanobacteria in preserved DNA isolated from lake sediments. Applied and Environmental Microbiology 77:8744–8753.

Schöne, H. K. 1982. The influence of light and temperature on the growth rates of six phytoplankton species from the upwelling area off Northwest Africa. Rapports et Proces-verbaux des Réunions. Conseil International pour l'Éxploration de la Mer 180:246–253.

Sherman, L. A., M. Connelly, and D. Sherman. 1976. Infection of *Synechococcus cedrorum* by the Cyanophage AS-1M. Virology 71:1–16.

Shirai, Y., Y. Takao, H. Mizumoto, Y. Tomaru, D. Honda, and K. Nagasaki. 2006. Genomic and phylogenetic analysis of a single-stranded RNA virus infecting *Rhizosolenia setigera* (Stramenopiles: Bacillariophyceae). Journal of the Marine Biological Association of the UK 86:475–483.

Shirai, Y., Y. Tomaru, Y. Takao, H. Suzuki, T. Nagumo, and K. Nagasaki. 2008. Isolation and characterization of a single-stranded RNA virus infecting the marine planktonic diatom *Chaetoceros tenuissimus* Meunier. Applied and Environmental Microbiology 74:4022–4027.

Simis, S. G. H., M. Tijdens, H. L. Hoogveld, and H. J. Gons. 2007. Optical signatures of the filamentous cyanobacterium *Leptolyngbya boryana* during mass viral lysis. Limnology and Oceanography 52:184–197.

Singh, P. K. 1974. Isolation and characterization of a new virus infecting the blue-green alga *Plectonema boryanum*. Virology 58:586–588.

Spilling, K., and S. Markager. 2008. Ecophysiological growth characteristics and modeling of the onset of the spring bloom in the Baltic Sea. Journal of Marine Systems 73:323–337.

Stoddard, L. I., J. B. H. Martiny, and M. F. Marston. 2007. Selection and characterization of cyanophage resistance in marine *Synechococcus* strains. Applied and Environmental Microbiology 73:5516–5522.

Strathmann, R. R. 1967. Estimating the organic carbon content of phytoplankton from cell volume or plasma volume. Limnology and Oceanography 12:411–418.

Šulčius, S., E. Šimoliunas, J. Staniulis, J. Koreivieňe, P. Baltrušis, R. Měskys, and R. Paškauskas. 2015. Characterization of a lytic cyanophage that infects the bloom-forming cyanobacterium *Aphanizomenon flos-aquae*. FEMS Microbiology Ecology 91:1–7.

Sule, P., and R. Belas. 2013. A novel inducer of *Roseobacter* motility is also a disruptor of algal symbiosis. Journal of Bacteriology 195:637–646.

Suttle, C. A., and A. M. Chan. 1993. Marine cyanophages infecting oceanic and coastal strains of *Synechococcus*: abundance, morphology, cross-infectivity and growth characteristics. Marine Ecology Progress Series 92:99–109.

Thompson, P., P. Harrison, and J. Parslow. 1991. Influence of irradiance on cell volume and carbon quota for ten species of marine phytoplankton. Journal of Phycology 27:351–360.

Tomaru, Y., N. Katanozaka, K. Nishida, Y. Shirai, K. Tarutani, M. Yamaguchi, and K. Nagasaki. 2004. Isolation and characterization of two distinct types of HcRNAV, a single-stranded RNA virus infecting the bivalve-killing microalga *Heterocapsa circularisquama*. Aquatic Microbial Ecology 34:207–218.

Tomaru, Y., Y. Shirai, H. Suzuki, T. Nagumo, and K. Nagasaki. 2008. Isolation and characterization of a new single-stranded DNA virus infecting the cosmopolitan marine diatom *Chaetoceros debilis*. Aquatic Microbial Ecology 50:103–112.

Tomaru, Y., Y. Shirai, K. Toyoda, and K. Nagasaki. 2011*a*. Isolation and characterisation of a single-stranded DNA virus infecting the marine planktonic diatom *Chaetoceros tenuissimus*. Aquatic Microbial Ecology 64:175–184.

Tomaru, Y., Y. Takao, H. Suzuki, T. Nagumo, K. Koike, and K. Nagasaki. 2011*b*. Isolation and characterization of a single-stranded DNA virus infecting *Chaetoceros lorenzianus* Grunow. Applied and Environmental Microbiology 77:5285–5293.

Tomaru, Y., Y. Takao, H. Suzuki, T. Nagumo, and K. Nagasaki. 2009. Isolation and characterization of a single-stranded RNA virus infecting the bloom-forming diatom *Chaetoceros socialis*. Applied and Environmental Microbiology 75:2375–2381.

Tomaru, Y., K. Toyoda, K. Kimura, Y. Takao, K. Sakurada, N. Nakayama, and K. Nagasaki. 2013*a*. Isolation and characterization of a single-stranded RNA virus that infects the marine planktonic diatom *Chaetoceros* sp. (SS08-C03). Phycological Research 61:27–36.

Tomaru, Y., K. Toyoda, H. Suzuki, T. Nagumo, K. Kimura, and Y. Takao. 2013*b*. New single-stranded DNA virus with a unique genomic structure that infects marine diatom *Chaetoceros setoensis*. Scientific Reports 3:3337.

Toyoda, K., K. Kimura, N. Hata, N. Nakayama, K. Nagasaki, and Y. Tomaru. 2012. Isolation and characterisation of a single-stranded DNA virus infecting the marine planktonic diatom *Chaetoceros* sp. (strain TG07-C28). Plankton and Benthos Research 7:20–28.

Van Etten, J. L., D. E. Burbank, Y. Xia, and R. H. Meints. 1983. Growth cycle of a virus, PBCV-1, that infects *Chlorella*-like algae. Virology 126:117–125.

Vaulot, D., J. Birrien, D. Marie, R. Casotti, M. J. W. Veldhuis, G. Kraay, and M. Chrétiennot-Dinet. 1994. Morphology, ploidy, pigment composition, and genome size of cultured strains of *Phaeocystis* (Prymnesiophyceae). Journal of Phycology 30:1022–1035.

Verity, P. G., C. Y. Robertson, C. R. Tronzo, M. G. Andrews, J. R. Nelson, and M. E. Sieracki. 1992. Relationships between cell volume and the carbon and nitrogen content of marine photosynthetic nanoplankton. Limnology and Oceanography 37:1434–1446.

Wang, K., and F. Chen. 2008. Prevalence of highly host-specific cyanophages in the estuarine environment. Environmental Microbiology 10:300–312.

Waters, R. E., and A. T. Chan. 1982. *Micromonas pusilla* virus: the virus growth cycle and associated physiological events within the host cells; host range mutation. Journal of General Virology 63:199–206.

Worden, A., J. Lee, and T. Mock. 2009. Green evolution and dynamic adaptations revealed by genomes of the marine picoeukaryotes *Micromonas*. Science 324:268–272.

Xia, H., T. Li, F. Deng, and Z. Hu. 2013. Freshwater cyanophages. Virologica Sinica 28:253–259.

Yamaguchi, H., S. Suzuki, Y. Tanabe, Y. Osana, Y. Shimura, K. Ishida, and M. Kawachi. 2015. Complete genome sequence of *Microcystis aeruginosa* NIES-2549, a bloom-forming cyanobacterium from Lake Kasumigaura, Japan. Genome Announcements 3:9–10.

Yamaguchi, M., S. Itakura, and T. Uchida. 2001. Nutrition and growth kinetics in nitrogen- or phosphorus-limited cultures of the "novel red tide" dinoflagellate *Heterocapsa circularisquama* (Dinophyceae). Phycologia 40:313–318.

Yan, X. D., T. Castberg, G. Bratbak, T. S. Baker, and P. R. Chipman. 2005. The marine algal virus PpV01 has an icosahedral capsid with T = 219 quasisymmetry. Journal of Virology 79:9236–9243.

Yoshida, T., Y. Takashima, Y. Tomaru, Y. Takao, S. Hiroishi, and Y. Shirai. 2006. Isolation and characterization of a cyanophage infecting the toxic cyanobacterium *Microcystis aeruginosa*. Applied and Environmental Microbiology 72:1239–1247.

Associate Editor: Spencer R. Hall
Editor: Alice A. Winn

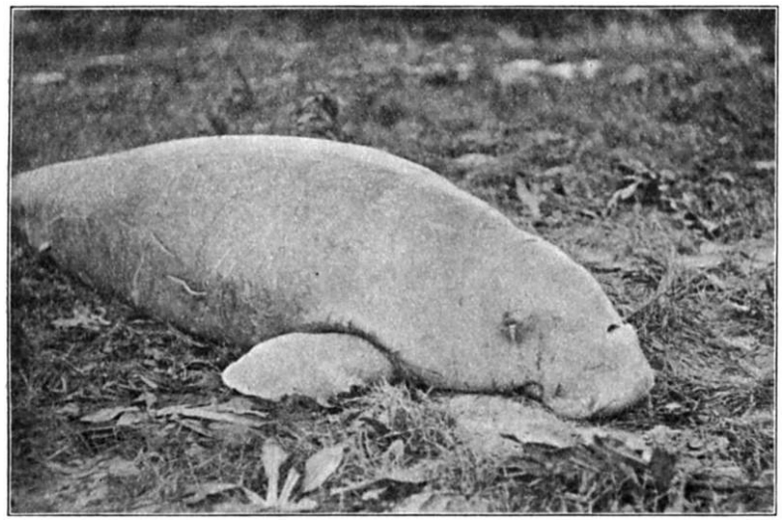

"As to the color of the dugong, Finsch has previously written at some length, and has brought together the various expressions that have been applied to this elusive shade. His account and that of Gill appear to agree with our own observations, namely, that the dorsal surface is in general a light grayish brown to bright bronze-brown with a slight metallic shimmer, while the ventral side is white to bright gray." From "External Morphology of the Dugong" by H. Dexler and L. Freund (*The American Naturalist*, 1906, 40:567–581).